

An ANFIS Regulator Integrated PQ Control of PV Array Connected Inverter for Grid Interconnection

Ramesh Nenavath¹, K. Krishnaveni², G. Mallesham³

¹ Research Scholar, Department of Electrical Engineering, University College of Engineering, Osmania University, Hyderabad, Telangana, India. Email: rameshn98@gmail.com

² Professor, Department of Electrical Engineering, Chaitanya Bharathi Institute of Technology, Hyderabad, Telangana, India

³ Professor, Department of Electrical Engineering, University College of Engineering, Osmania University, Hyderabad, Telangana, India

ARTICLE INFO	ABSTRACT
Received: 18 April 2025	<p>With the growing concern over global warming, the frequency of climate-related disasters is steadily increasing worldwide. A major contributor to this issue is environmental pollution caused by carbon emissions from non-renewable energy sources. To address this, renewable energy sources, which harness natural resources for power generation, are becoming essential. Among these, PV arrays are the most prominent, utilizing solar irradiation to generate electrical energy. In conventional PV systems, the inverter typically employs a SRF controller, which lacks the ability to regulate active and reactive power injection effectively. To overcome this limitation, the SRF controller is replaced with a PQ controller, which enables precise control over both active and reactive power flows. The PQ control strategy employs a dual-loop structure: the active power loop regulates the d-axis component, while the reactive power loop governs the q-axis component. Reference current components are generated using individual regulators, typically implemented as PI controllers. However, due to the low damping and linear characteristics of PI regulators, they are not well-suited for systems subjected to non-linear disturbances. To enhance system performance, this paper proposes replacing the conventional PI regulator with FL and ANFIS regulators. A comparative analysis is conducted, evaluating voltage profiles, power injection, and THD levels across these control strategies. The analysis identifies the most effective regulator for optimal PQ control in inverter-based PV systems.</p> <p>Keywords: PV (Photo Voltaic), SRF (Synchronous Reference Frame), PQ (Active and Reactive powers), PI (Proportional Integral), FL (Fuzzy Logic), ANFIS (Adaptive Neuro Fuzzy Inference System), THD (Total Harmonic Distortion).</p>
Revised: 28 May 2025	
Accepted: 12 Jun 2025	

INTRODUCTION

The rise in carbon emissions resulting from electricity generation using fossil fuels and nuclear energy has significantly contributed to environmental pollution and global warming [1]. This global warming, in turn, has triggered catastrophic climate events, leading to widespread property damage and increased loss of life [2] [3]. To mitigate these adverse effects, conventional power generation methods must be replaced with cleaner, renewable energy sources.

Among the available renewable options—such as wind farms, tidal energy systems, and biogas plants—solar power stands out as the most reliable and easily deployable solution [4]. Solar power systems use PV panels to harness solar radiation and generate electrical energy. These PV panels are typically configured in series-parallel combinations to achieve the required power output [5]. The generated DC voltage is then processed through one or more boost converters, which operate in parallel to extract maximum power and increase voltage levels.

This boosted DC voltage must be converted into AC for practical use. Single-phase inverters are used for residential installations, while three-phase inverters are necessary for grid-connected systems with higher power ratings [6]. In grid-connected applications, the inverter must operate in synchronization with the grid to ensure stable power sharing without introducing disturbances or harmonics.

Traditionally, the SRF technique is employed to control the inverter using feedback from grid voltages [7]. However, the SRF method assumes the q-axis current component to be zero, implying no reactive power exchange between the inverter and the grid. This approach places the entire burden of reactive power compensation on the grid, potentially lowering its power factor.

For improved performance, it is essential to manage both active and reactive power flows through the inverter [8]. Reactive power injection from the PV system can offset a portion of the load's reactive power demand, thereby enhancing the grid's power factor. Since the SRF controller only regulates the d-axis current component, it falls short in this regard.

To overcome these limitations, a Grid-Forming (GFL) controller based on the PQ control approach is proposed [9]. This controller uses real-time feedback from both grid voltages and inverter currents to generate reference signals for active and reactive power injection. These signals are then used to produce gating pulses for the inverter using the Sinusoidal Pulse Width Modulation (SPWM) technique. The overall architecture of the proposed grid-connected inverter system is illustrated in Figure 1.

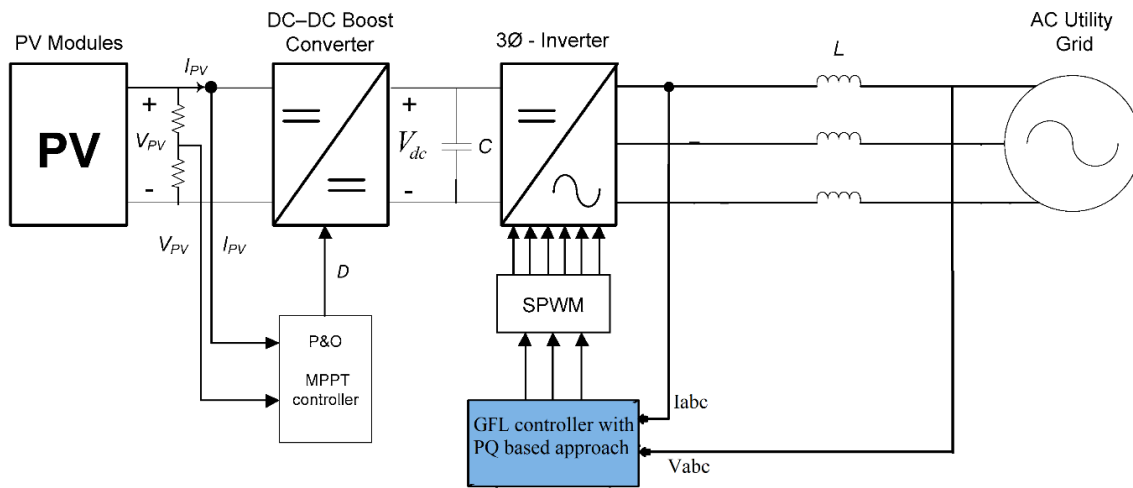


Figure 1: Outline structure of the proposed system

As illustrated in Figure 1, the photovoltaic (PV) modules are connected to a DC-DC boost converter, which is operated using the Perturb and Observe (P&O) Maximum Power Point Tracking (MPPT) technique. This MPPT algorithm generates a duty cycle (D) that is compared with a high-frequency sawtooth waveform to produce the gating pulse for the boost converter switch. The output of the boost converter is then fed to a three-phase inverter, which is controlled by a Grid-Forming (GFL) controller implementing a PQ-based control strategy [10].

The GFL controller employs a dual-loop structure to regulate both active and reactive power. The active power loop governs the d-axis current component, while the reactive power loop controls the q-axis component. Each loop uses a Proportional-Integral (PI) regulator to generate the corresponding reference current components. However, due to the low damping nature of PI regulators, the system may experience significant oscillations and harmonic distortion, especially under dynamic or non-linear conditions.

To address these limitations, advanced control strategies using Fuzzy Logic and Adaptive Neuro-Fuzzy Inference System (ANFIS) regulators are introduced for reference signal generation [11]. These intelligent controllers are more effective in handling system non-linearities and disturbances. Instead of producing large transient peaks, they offer smoother responses, minimizing overshoot and improving system damping. As a result, inverter performance is enhanced with reduced oscillations and improved stability, effectively achieving a critically damped response.

The structure of this paper is organized as follows:

- **Section 1** introduces the proposed renewable energy system, outlining its configuration and key components.

- **Section 2** details the system configuration, circuit topology, and control design of both the boost converter and the inverter.
- **Section 3** focuses on the design of the ANFIS regulator, including the definition of input and output membership functions (MFs), rule base, and training using a backpropagation optimization technique.
- **Section 4** presents the simulation results and analysis of the system performance using PI, Fuzzy Logic, and ANFIS controllers. A comparative evaluation is conducted based on key performance parameters such as voltage, power output, and total harmonic distortion (THD).
- **Section 5** concludes the paper by summarizing findings and validating the most effective regulator for the proposed system. References cited throughout the work follow this section.

SYSTEM CONFIGURATION

As outlined earlier in Section 1, the solar plant operates through a two-stage power conversion process: maximum power extraction and inversion. Maximum power extraction is carried out using an MPPT technique that controls the switching of the boost converter. This boost converter not only facilitates power tracking but also steps up the PV array voltage by approximately 2 to 2.5 times, depending on system requirements. Voltage boosting is achieved through a series-connected storage inductor, which is sized based on the PV array's power rating [12]. To minimize voltage ripple at the output, a capacitor is incorporated and designed in accordance with the allowable ripple limits. The required inductance and capacitance values for the boost converter are given as follows:

$$L_b = \frac{R_L D (1-D)^2}{2 f_s} \quad (1)$$

$$C_o = \frac{V_o \cdot D}{f_s \cdot \Delta V_o \cdot R_L} \quad (2)$$

Here, D is the duty ratio of the switch determined by the P&O MPPT technique, f_s is the switching frequency of the switch, V_o is the output DC voltage, ΔV_o allowable voltage ripple % and R_L is the load resistance calculated as

$$R_L = \frac{P_{pv}^2}{V_o} \quad (3)$$

Using the values derived from the PV array's power rating, the boost converter is appropriately designed and operated. At its output, a six-switch inverter is connected to convert the boosted DC voltage into a two-level, three-phase AC voltage [13]. This inverter is driven using the Sin PWM technique, which generates switching pulses based on the reference signals provided by the GFL controller employing a PQ-based approach. The generation of Sin PWM pulses is illustrated in Figure 2.

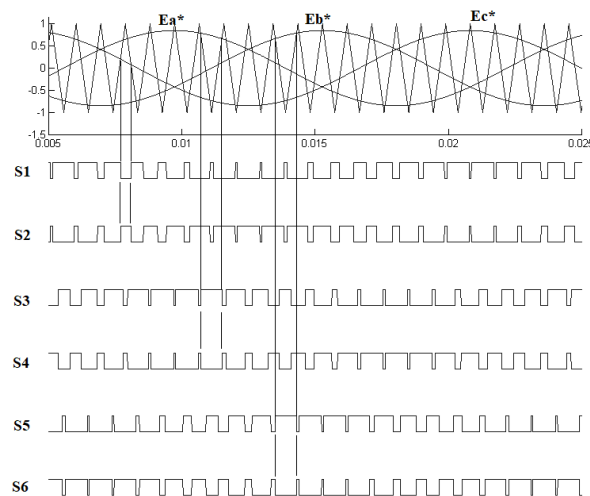


Figure 2: Sin PWM technique pulse generation

As shown in Figure 2, the three reference sinusoidal signals E_a^* , E_b^* and E_c^* are compared with a high-frequency triangular carrier waveform to generate gate pulses for the upper switches S_1 , S_3 and S_5 of the inverter [14] [15]. The corresponding lower switches S_2 , S_4 and S_6 receive their gate pulses through NOT gates, ensuring that both switches in the same inverter leg are not turned ON simultaneously, thereby preventing short circuits. The complete circuit diagram of the proposed system including PV panels, the boost converter, and the inverter connected to the grid is shown in Figure 3.

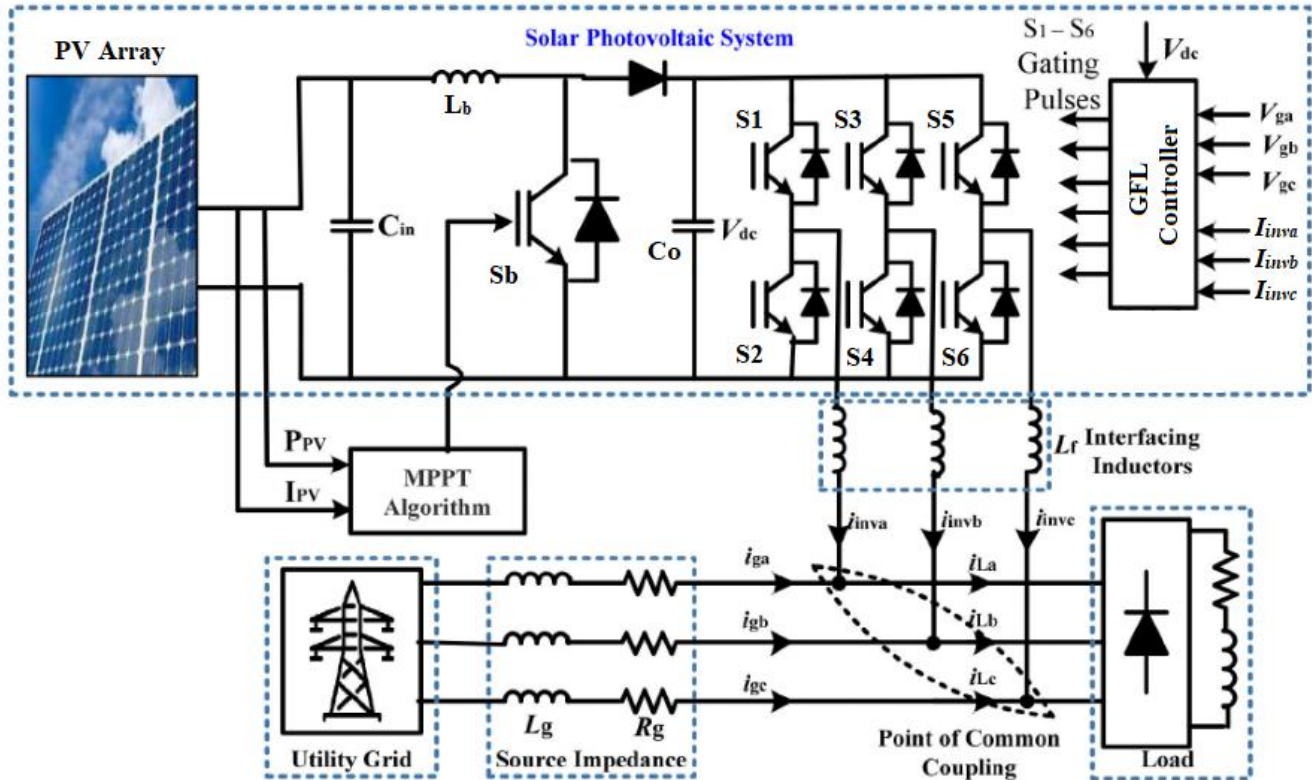


Figure 3: Grid connected PV array circuit topology

As illustrated in Figure 3, the GFL with PQ control controller regulates the six inverter switches using feedback from the grid voltages and inverter output currents [16]. The detailed internal structure of the GFL controller used for inverter control is depicted in Figure 4.

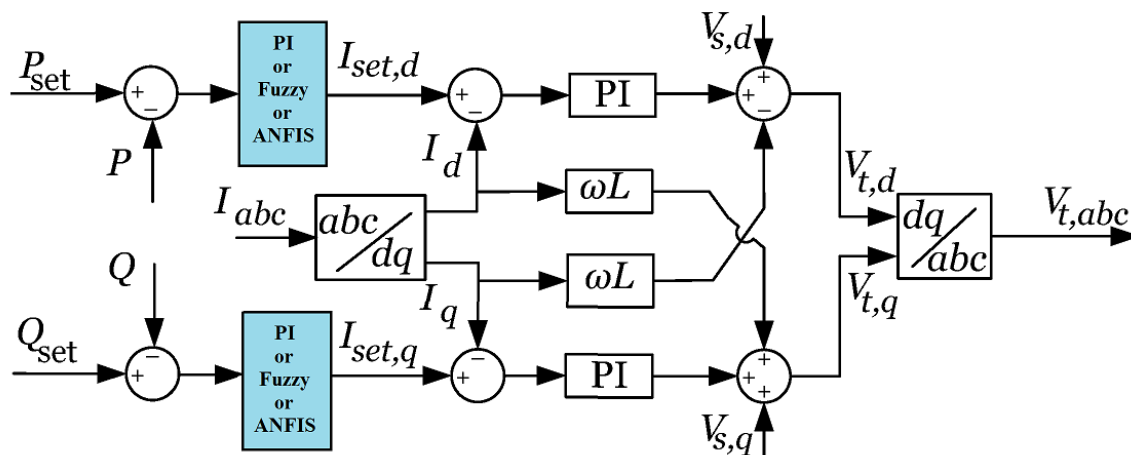


Figure 4: GFL internal structure

The reference dq current components are generated by the active and reactive power regulators which are conventional PI regulator [17]. The reference dq current components are generated by the given expressions

$$I_{set,d} = (P_{set} - P) \left(k_p + \frac{k_i}{s} \right) \quad (4)$$

$$I_{set,q} = (Q_{set} - Q) \left(k_p + \frac{k_i}{s} \right) \quad (5)$$

Here, P_{set} and P are the set point and actual active powers, Q_{set} and Q are the set point and actual reactive powers, k_p and k_i are the proportional and integral gains of the PI regulator [18]. Due to the disadvantages of the PI regulator, it is replaced with advanced regulators Fuzzy Logic and ANFIS modules. The Fuzzy Logic regulator has two inputs and one output variables which are defined to be error (e), change in error (ce) and $I_{set,dq}$ components respectively [19]. The Fuzzy Logic module has multiple membership functions included in specific ranges as per the input values. The Fuzzy membership functions of the input and output variables is presented in figure 5.

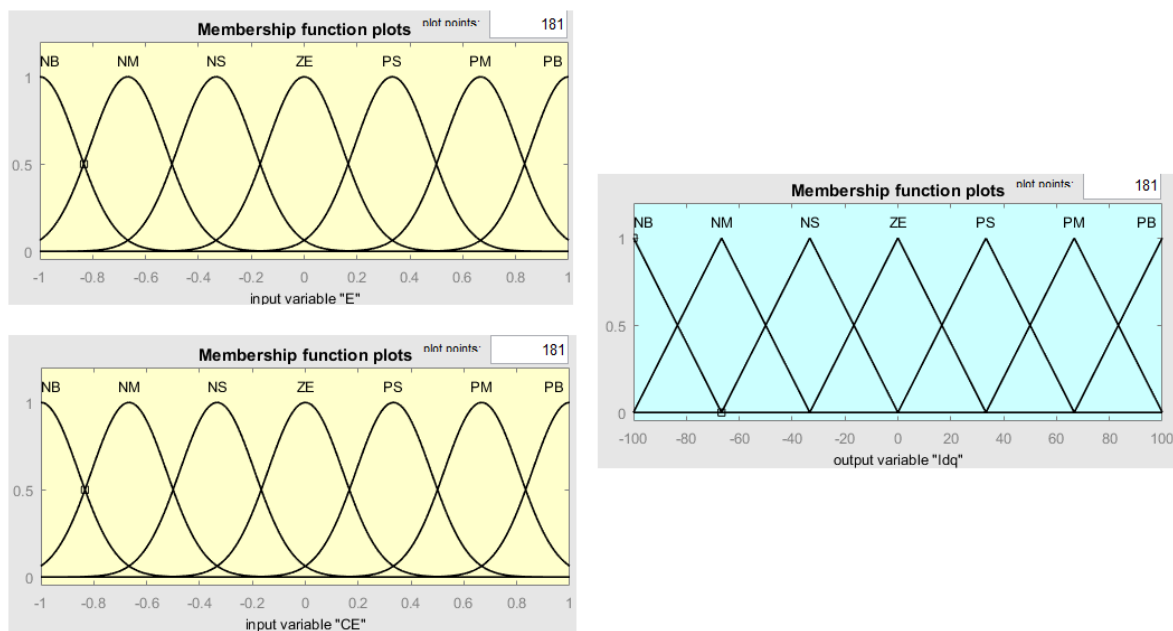


Figure 5: Membership functions of the input and output variables

The output of the Fuzzy Logic module is generated by the rule base set as per the position of the value in the membership functions [20]. The rule base for the generation of dq current components is given in table 1.

Table 1: Fuzzy module Rule base

e \ ce	NB	NM	NS	ZE	PS	PM	PB
PB	Z	PS	PM	PB	PB	PB	PB
PM	NS	Z	PS	PM	PB	PB	PB
PS	NB	NS	Z	PS	PM	PB	PB
ZE	NB	NM	NS	Z	PS	PM	PB
NS	NB	NB	NM	NS	Z	PS	PM
NM	NB	NB	NB	NM	NS	Z	PS
NB	NB	NB	NB	NB	NM	NS	Z

From the $i_{set,dq}$ components the reference $V_{t,dq}$ components are generated as

$$V_{t,d} = V_{s,d} + (I_{set,d} - I_d) \left(k_{pv} + \frac{k_{iv}}{s} \right) - I_q \omega L \quad (6)$$

$$V_{t,q} = V_{s,q} + (I_{set,q} - I_q) \left(k_{pv} + \frac{k_{iv}}{s} \right) + I_d \omega L \quad (7)$$

Here, $V_{s,dq}$ and I_{dq} are the actual dq grid voltage and inverter current components respectively generated by the Park's transformation equations, k_{pv} and k_{iv} are the voltage regulator proportional and integral gains, ω are the angular frequency of the grid voltage and L is the filter inductance between inverter and grid. The final generated signals $V_{s,dq}$ are converted to reference Sin signals (E_a^* , E_b^* and E_c^*) using inverse Park's transformation. The $I_{set,dq}$ components can further be tuned with better response using ANFIS regulator which is more adaptive to the disturbance caused in the system.

ANFIS DESIGN

The ANFIS regulator used for generating the d and q current components is based on the 'Sugeno' fuzzy inference model and utilizes seven membership functions. It is designed with one input variable (error) and one output variable (either d or q) [21]. The input membership functions are of triangular type and defined over a specified range in per-unit (p.u.) format. The output membership functions are linear and assigned fixed numerical values. While the output functions remain constant, the input membership functions are adaptively tuned based on the training data obtained from the previously used regulator [22]. Figure 6 illustrates the input and output membership functions of the Sugeno-type ANFIS system.

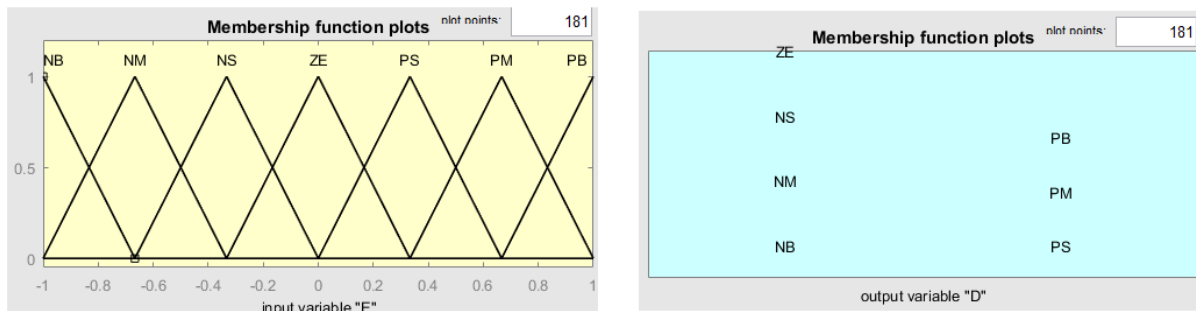


Figure 6: ANFIS input and output variables membership functions

The input variable is defined over a range of -1 to +1, representing the per-unit error obtained by comparing the reference and actual power values. The output variable has a range from -10 to +10, determined based on the controller's response [23]. The output membership functions are assigned fixed values: NB (-10), NM (-6.6), NS (-3.3), ZE (0), PS (3.3), PM (6.6), and PB (10). These ANFIS membership functions are trained using input-output data collected from the PI regulator [24]. The training process employs the 'backpropagation' optimization algorithm available within the Fuzzy ANFIS tool. Figure 7 shows the trained and imported data used in the ANFIS model.

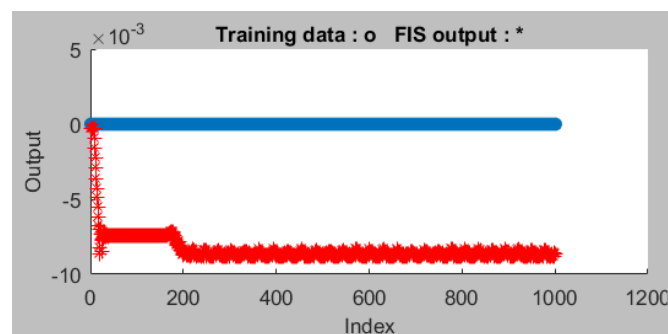


Figure 7: Trained data using ANFIS tool

The trained FIS structure is exported to the workspace using the Fuzzy tool and integrated into the GFL controller for generating the d-q current components. By applying neuro-training on the PI regulator data using the backpropagation algorithm, the generated d-q components exhibit reduced disturbances and oscillations, leading to improved reference signal generation [25]. The performance of the system with the updated regulators, under the same system rating, is analysed in the following section.

RESULTS AND DISCUSSION

The simulation of the proposed system which include PV array connected to boost converter for maximum power extraction interconnection to grid through inverter is modelled using Simulink tools. The blocks from the 'Electrical' module which include 'Sources', 'Power electronics', 'Passives', and 'measurements' subsets are used for the designing. The Simulink blocks imported into the design are updated with the simulation parameters as per table 2.

Table 2: System parameters

Name of the module	Parameters
PV plant	$V_{mp} = 30.1V$, $I_{mp} = 8.3A$, $V_{oc} = 37.2V$, $I_{sc} = 8.87A$, $N_p = 200$, $N_s = 24$. $P_{pv\ total} = 1.2MW$.
Boost converter	$L_b = 5mH$, $C_{in} = 100\mu F$, $C_{out} = 12000\mu F$.
MPPT	$\Delta D = 0.05$, MPPT gain = 5, $D_{int} = 0.5$, $f_s = 5kHz$.
Grid	132kV, 50Hz, 2500MVA.
Inverter	1.2MVA, 400V, 50Hz, $f_c = 2kHz$. Filter – $L_f = 250\mu H$, $C_f = 100kVAR$.
PQ control	PI regulator - $K_p = 0.023$, $K_i = 0.005$, $K_{pi} = 0.5$, $K_{ii} = 0.001$ Fuzzy Logic – 'e' range = -200 to 200, 'de' range = -1 to 1 and Idqref range = -50 to 50.

The system is updated with the specified parameters, and the simulation is carried out for 2 seconds using reference values of $P_{set} = 0.9pu$ and $Q_{set} = -0.4 pu$. The simulation incorporates PI, Fuzzy Logic, and ANFIS regulators within the GFL controller to enable a comparative performance analysis. This section presents the comparison results of voltage profiles, power output, frequency response, and current THD for the different control strategies. As illustrated in Figure 8, the DC link voltage measured at the output of the boost converter shows notable differences across the three regulators. For the given set points, the PI regulator exhibits a peak overshoot of 3700 V, while the Fuzzy Logic controller reduces it to 3000 V. The ANFIS regulator significantly minimizes the overshoot to just 1300 V, indicating its superior control performance. Furthermore, the settling time is improved from 0.5 s with the PI regulator and 0.4 s with Fuzzy Logic to 0.3 s with the ANFIS controller. These improvements demonstrate the robustness and effectiveness of the ANFIS-based regulator in managing the system's initial transients and enhancing overall stability.

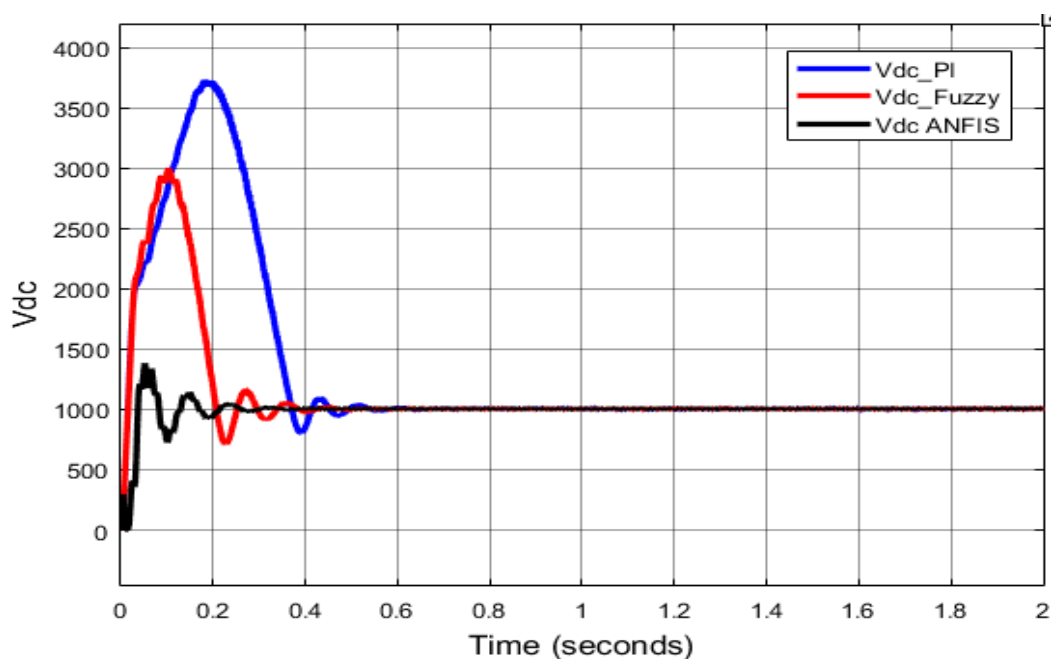


Figure 8: DC link voltage comparison

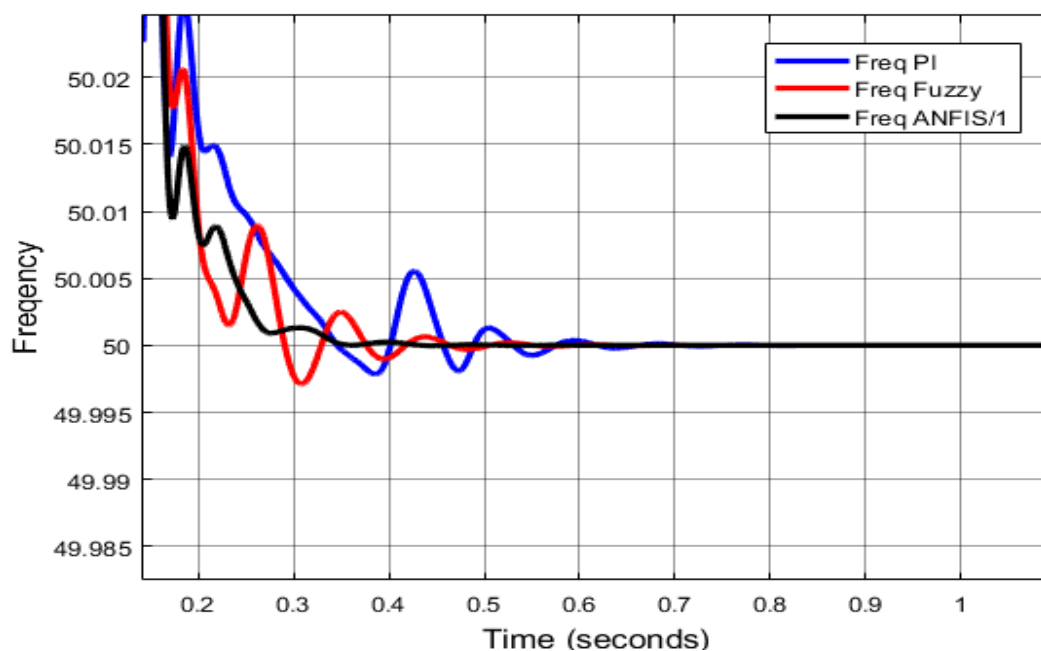


Figure 9: PCC voltage frequency comparison

The ANFIS regulator also enhances the frequency settling time at the PCC, where the inverter interfaces with the grid. With the PI regulator, the frequency settles at 0.6 s, while the Fuzzy regulator improves it to 0.5 s. The ANFIS regulator further reduces the settling time to 0.4 s, contributing to a faster and more stable system response. This improvement directly influences the performance of active and reactive power injection, as illustrated in Figure 10. The comparison of active and reactive power responses reveals significant reductions in both initial peak overshoot and settling time. Active power with the ANFIS controller settles in just 0.3 s, compared to 0.5 s with the PI regulator and 0.4 s with the Fuzzy controller. Similarly, the reactive power peak overshoot is reduced from 1.6 pu (PI) and 1.3 pu (Fuzzy) to just 0.7 pu with ANFIS. These results clearly demonstrate the superior dynamic performance and control precision offered by the ANFIS-based regulator.

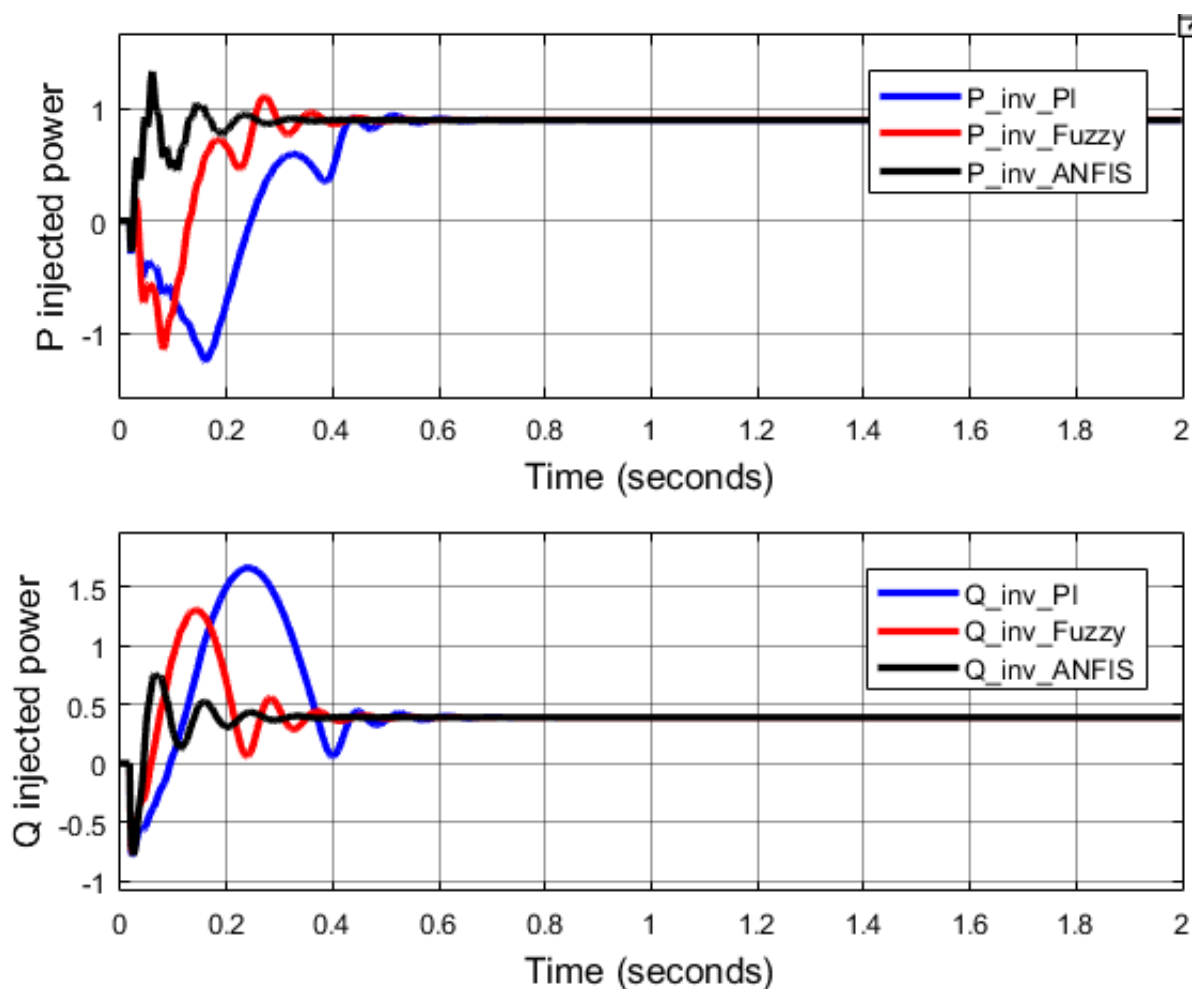
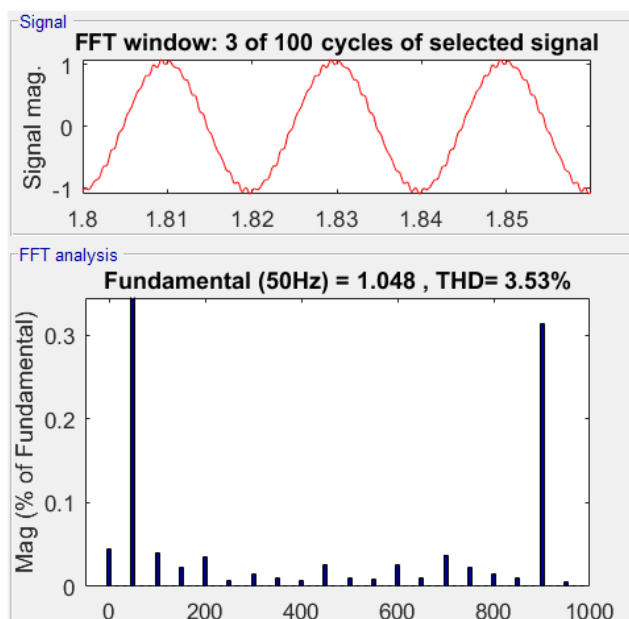
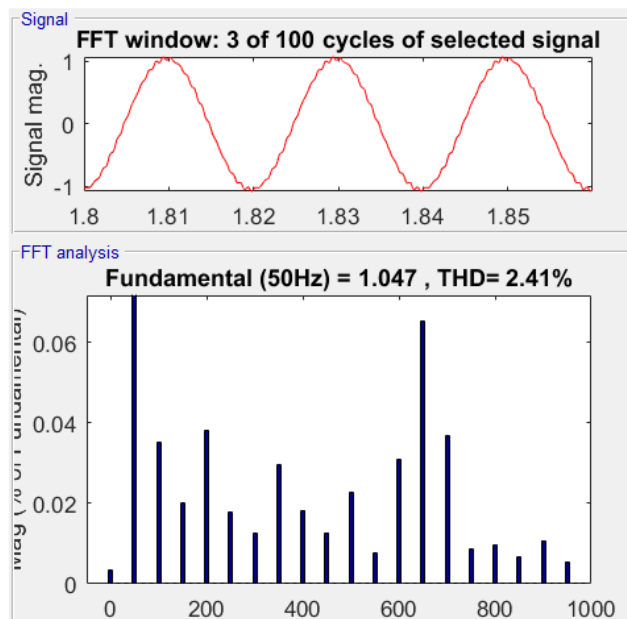


Figure 10: Active and Reactive powers comparison



(a)



(b)

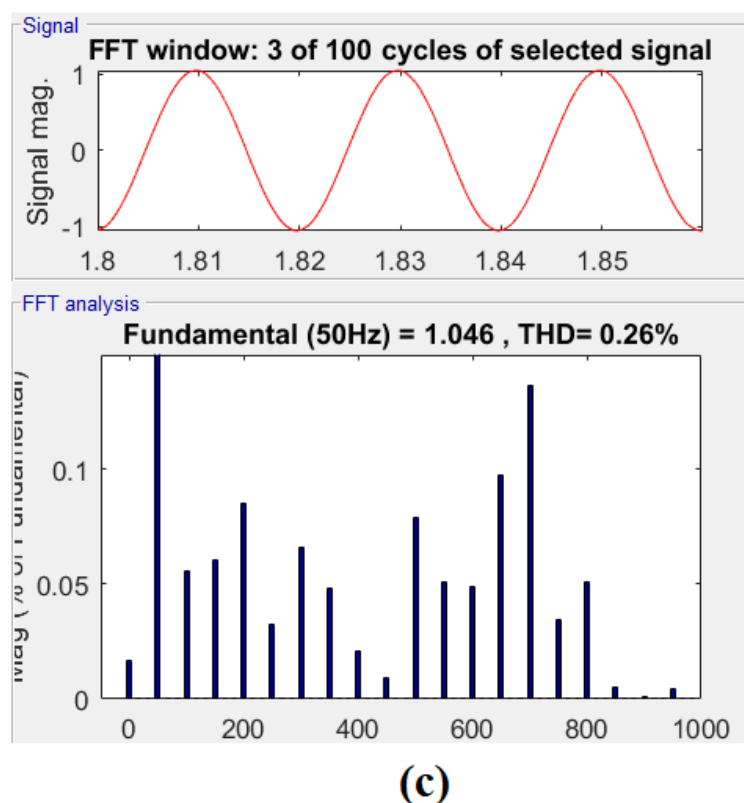


Figure 11: THD of inverter current (a) PI regulator (b) Fuzzy Logic regulator (c) ANFIS regulator

In the final parametric comparison, the THD of the inverter current is significantly reduced to just 0.26% with the ANFIS regulator, compared to 3.53% with the PI regulator and 2.41% with the Fuzzy controller. This substantial reduction highlights the enhanced performance of the inverter when the GFL controller is equipped with an optimized adaptive regulator. Table 3 presents a summary of the key performance parameters for each regulator implemented within the GFL control structure.

Table 3: Parametric comparison table

Name of the parameter	PI regulator	Fuzzy Logic regulator	ANFIS regulator
DC voltage peak overshoot	3700V	3000V	1300V
DC voltage settling time	0.5sec	0.4sec	0.3sec
Frequency settling time	0.6sec	0.5sec	0.4sec
P settling time	0.5sec	0.4sec	0.3sec
Q settling time	0.6sec	0.4sec	0.3sec
Q initial peak	1.6pu	1.3pu	0.7pu
Current THD	3.53%	2.41%	0.26%

CONCLUSION

In conclusion, this study highlights the limitations of traditional SRF and PI-based control strategies in inverter-based PV systems, particularly under non-linear and dynamic operating conditions. By implementing advanced control techniques such as Fuzzy Logic (FL) and Adaptive Neuro-Fuzzy Inference System (ANFIS) regulators within the PQ control framework, the system demonstrates significant improvements in power quality and control accuracy.

The comparative analysis confirms that the proposed intelligent regulators enhance voltage stability, optimize active and reactive power injection, and reduce total harmonic distortion (THD). Thus, FL and ANFIS-based PQ controllers offer a robust and efficient solution for modern renewable energy systems, supporting cleaner and more reliable grid integration of photovoltaic power.

REFERENCES

- [1] Muhammad Kabir, Um E Habiba, Wali Khan, Amin Shah, Sarvat Rahim, Patricio R. De los Rios-Escalante, Zia-Ur-Rehman Farooqi, Liaqat Ali, Muhammad Shafiq, "Climate change due to increasing concentration of carbon dioxide and its impacts on environment in 21st century; a mini review," *Journal of King Saud University - Science*, Volume 35, Issue 5, 2023, 102693, ISSN 1018-3647, <https://doi.org/10.1016/j.jksus.2023.102693>.
- [2] Abbass, K., Qasim, M.Z., Song, H. *et al.* A review of the global climate change impacts, adaptation, and sustainable mitigation measures. *Environ Sci Pollut Res* **29**, 42539–42559 (2022). <https://doi.org/10.1007/s11356-022-19718-6>
- [3] Akkari C, Bryant CR (2016) The co-construction approach as approach to developing adaptation strategies in the face of climate change and variability: A conceptual framework. *Agricultural Research* 5(2):162–173
- [4] A.G. Olabi, Mohammad Ali Abdelkareem, "Renewable energy and climate change," *Renewable and Sustainable Energy Reviews*, Volume 158, 2022, 112111, ISSN 1364-0321, <https://doi.org/10.1016/j.rser.2022.112111>.
- [5] K.N. Nwaigwe, P. Mutabilwa, E. Dintwa, "An overview of solar power (PV systems) integration into electricity grids," *Materials Science for Energy Technologies*, Volume 2, Issue 3, 2019, Pages 629-633, ISSN 2589-2991, <https://doi.org/10.1016/j.mset.2019.07.002>.
- [6] M. Shafiullah, S. D. Ahmed and F. A. Al-Sulaiman, "Grid Integration Challenges and Solution Strategies for Solar PV Systems: A Review," in *IEEE Access*, vol. 10, pp. 52233-52257, 2022, doi: 10.1109/ACCESS.2022.3174555.
- [7] A. Patel, H. Datt Mathur and S. Bhanot, "A new and simple SRF based power angle control for UPQCdg to integrate solar PV into grid," *2017 7th International Conference on Power Systems (ICPS)*, Pune, India, 2017, pp. 75-80, doi: 10.1109/ICPES.2017.8387271.
- [8] Aldbaiat, B.; Nour, M.; Radwan, E.; Awada, E. Grid-Connected PV System with Reactive Power Management and an Optimized SRF-PLL Using Genetic Algorithm. *Energies* **2022**, *15*, 2177. <https://doi.org/10.3390/en15062177>
- [9] P. P. Waghmare, S. Y. Gadgune and P. S. Rajmane, "Solar Energy Integration Using Grid Forming Inverter," *2023 IEEE Engineering Informatics*, Melbourne, Australia, 2023, pp. 1-5, doi: 10.1109/IEEECONF58110.2023.10520482.
- [10] Muhammad Akbar Syahbani, Makbul Anwari Muhammad Ramli, Prisma Megantoro, Alfananda Ardiansyah, Intan Dwi Cahyani, Noer Fadzri Perdana Dinata, Rifqi Firmansyah, Muhammad Zohri, Firmansyah Nur Budiman, "Performance enhancement of grid-forming inverter-controlled PV systems: A comparative study with and without battery energy storage under intermittent and unbalanced load conditions," *Results in Engineering*, Volume 27, 2025, 105980, ISSN 2590-1230, <https://doi.org/10.1016/j.rineng.2025.105980>.
- [11] Srimatha, S., Mallala, B. & Upendar, J. A novel ANFIS-controlled customized UPQC device for power quality enhancement. *Journal of Electrical Systems and Inf Technol* **10**, 55 (2023). <https://doi.org/10.1186/s43067-023-00121-1>
- [12] Ansari, S.; Chandel, A.; Tariq, M. A Comprehensive Review on Power Converters Control and Control Strategies of AC/DC Microgrid. *IEEE Access* **2021**, *9*, 17998–18015.
- [13] Tsai, C.H., Figueroa-Acevedo, A., Boese, M., et al.: Challenges of planning for high renewable futures: experience in the U.S. midcontinent electricity market. *Renewable Sustainable Energy Rev.* **131**, 1–14 (2020)

- [14] Sajadi, A., Kenyon, R.W., Hodge, B.-M.: Synchronization in electric power networks with inherent heterogeneity up to 100% inverter-based renewable generation. *Nat. Commun.* **13**(1), 2490 (2022)
- [15] Ward, L.; Subburaj, A.; Demir, A.; Chamana, M.; Bayne, S.B. Analysis of Grid-Forming Inverter Controls for Grid-Connected and Islanded Microgrid Integration. *Sustainability* **2024**, *16*, 2148. <https://doi.org/10.3390/su16052148>
- [16] Du, W.; Tuffner, F.K.; Schneider, K.P.; Lasseter, R.H.; Xie, J.; Chen, Z.; Bhattarai, B. Modeling of grid-forming and grid-following inverters for dynamic simulation of large-scale distribution systems. *IEEE Trans. Power Deliv.* **2020**, *36*, 2035–2045.
- [17] Hadjileonidas, A.; Li, Y.; Green, T.C. Comparative analysis of transient stability of grid-forming and grid-following inverters. In Proceedings of the 2022 IEEE International Power Electronics and Application Conference and Exposition (PEAC), Guangzhou, China, 4–7 November 2022; pp. 296–301.
- [18] Bahrani, B. Power-Synchronized Grid-Following Inverter Without a Phase-Locked Loop. *IEEE Access* **2021**, *9*, 112163–112176.
- [19] Hannan MA, Ghani ZA, Hoque MM, Ker PJ, Hussain A, Mohamed A (2019) Fuzzy logic inverter controller in photovoltaic applications: issues and recommendations. *IEEE Access* *7*:24934–24955
- [20] Kerdphol T, Watanabe M, Hongesombut K, Mitani Y (2019) Self-adaptive virtual inertia control-based fuzzy logic to improve frequency stability of microgrid with high renewable penetration. *IEEE Access* *7*:76071–76083
- [21] Osheba, D.S.M., Osheba, S.M., Nazih, A. *et al.* Performance enhancement of PV system using VSG with ANFIS controller. *Electr Eng* **105**, 2523–2537 (2023).
- [22] ANFIS Control of PV Tied Grid System with Multi-Carrier PWM-Based Modular 5-Level Converter," *SSRG International Journal of Electrical and Electronics Engineering*, vol. 9, no. 12, pp. 145-155, 2022. <https://doi.org/10.14445/23488379/IJEEE-V9I12P113>
- [23] Bilgundi, S.K., Sachin, R., Pradeepa, H. *et al.* Grid power quality enhancement using an ANFIS optimized PI controller for DG. *Prot Control Mod Power Syst* *7*, 3 (2022). <https://doi.org/10.1186/s41601-022-00225-2>
- [24] Bilgundi, S.K., Sachin, R., Pradeepa, H. *et al.* Grid power quality enhancement using an ANFIS optimized PI controller for DG. *Prot Control Mod Power Syst* *7*, 3 (2022). <https://doi.org/10.1186/s41601-022-00225-2>
- [25] Vaishali Chavhan, Mukesh Kumar, Sarvesh Kumar, Chetan Bobade, "ANFIS Hybridized FACTS Controller for Voltage Stability Improvement," *SSRG International Journal of Electronics and Communication Engineering*, vol. 12, no. 1, pp. 150-160, 2025. <https://doi.org/10.14445/23488549/IJECE-V12I1P112>